

Central European Journal of Chemistry

Aqueous phenol and ethylene glycol solutions in electrohydrodynamic liquid bridging

Invited Paper

Mathias Eisenhut^{1,2}, Xinghua Guo², Astrid H. Paulitsch-Fuchs¹, Elmar C. Fuchs^{1,*}

¹Wetsus – Centre of Excellence for Sustainable Water Technology, 8900 CC Leeuwarden, The Netherlands

²Institute of Analytical Chemistry and Food Chemistry, Graz University of Technology, 8010 Graz, Austria

Received 30 November 2010; Accepted 10 February 2011

Abstract: The formation of aqueous bridges containing phenol and ethylene glycol as well as bisphenol-A, hydrochinone and p-cresol under the application of high voltage DC ("liquid bridges") is reported. Detailed studies were made for phenol and glycol with concentrations from 0.005 to 0.531 mol L-1. Conductivity as well as substance and mass transfers through these aqueous bridges are discussed and compared with pure water bridges. Previously suggested bidirectional mass transport is confirmed for the substances tested. Anodic oxidation happens more efficiently when phenol or glycol are transported from the cathode to the anode since in this case the formation of a passivation layer or electrode poisoning are retarded by the electrohydrodynamic (EHD) flow. The conductivity in the cathode beaker decreases in all experiments due to electrophoretic transport of naturally dissolved carbonate and bicarbonate to the anode. The observed electrochemical behavior is shortly discussed and compared to known mechanisms.

Keywords: Floating water bridge • Electrohydrodynamics • Phenol oxidation • Glycol oxidation

© Versita Sp. z o.o.

1. Introduction

In 1893, Sir William Armstrong placed a cotton thread between two wine glasses filled with chemically pure water. After applying a high voltage, a watery connection formed between the two glasses, and after some time, the cotton thread was pulled into one of the glasses, leaving, for a few seconds, a rope of water suspended between the lips of the two glasses [1]. Although easy to reproduce, this watery connection with more or less cylindrical shape between the two beakers, henceforth referred to as 'water bridge', holds a number of interesting static and dynamic phenomena [2-7].

Molecular and nanoscale field-induced formations of liquid bridges of ethanol have been investigated in the framework of silicon carbide nanowire fabrication [8]; a molecular mechanism of the formation of a nanoscale water pillar has been presented [9]. On a macroscopic level, several of these phenomena can be explained by modern electrohydrodynamics, analyzing the motion of fluids in electric fields (see, e.g. the Maxwell pressure tensor considerations by Widom et al. [10], or the book

of Castellanos [11]), while on the molecular scale water can be described by quantum mechanics (e.g. [12,13]). The gap at the mesoscopic scale is bridged by a number of theories including quantum mechanical entanglement and coherent structures in water, theories which are currently discussed (e.g. [14-18] for water in general, and [19] specifically for the water bridge). Previous experiments [2] suggested a possible change of the water microstructure inside the water bridge; first neutron scattering experiments [4] showed no difference in the microdensity of a D₂O bridge compared to the bulk; recent 2D neutron scattering experiments [5] indicated a preferred molecular orientation within a floating heavy water bridge; detailed optical investigations [6] suggested the existence of a mesoscopic bubble network within the water bridge; and a Raman scattering study on vertical water bridges reported on a polarized water structure induced by the electric field [20]. There is a comprehensive review about water bridge research [21] comprising its most important features, and the behavior of the phenomenon under low gravity conditions has been investigated recently [22].

^{*} E-mail: elmar.fuchs@wetsus.nl

The properties of water at mesoscopic scales have drawn special attention due to their suggested relevance to human physiology [23].

Recently, the mechanism of charge storage and transfer in water in general has been reevaluated [24] and intensely discussed [25-27]. From the previous water bridge investigations [2-6] charge transport and possible nano-bubble formation in this experiment remains to be satisfactorily explained. Another recent study [28] indicates the existence of a mesoscopic charge and mass and transport mechanism in pure water.

As far as the basic mechanism of the water-bridge formation is concerned, the phenomenon is well-established [21] and was explained in some recent papers using simple schemes [29-31]. According to those schemes, the most important properties necessary for a liquid bridge formation are high dielectric permittivity, low electric conductivity and a permanent molecular dipole moment. Thus the phenomenon is not water-specific but can be reproduced with any liquid of similar properties like methanol [21] or glycerol [30].

One feature which is not very well understood is the electrochemical behavior. Although there is a significant current flow, electrolysis is not observed [2-6], and the addition of substances which increase the conductivity like salts [7] or pH dyes [28] destabilizes the bridge and promotes electrochemical reactions. So far, the electrochemistry of non-ionic solvents has not been investigated in the set-up described. This work intends to start filling this gap. Therefore, the high voltage electrochemistry of phenol and ethylene glycol was investigated. Since the anodic oxidation of phenol is very well-studied due to its importance in waste water treatment [32-40], its electrochemical behavior is very well known. Therefore it was chosen as sample substance. For comparative reasons, the behavior of the simple aliphatic alcohol ethylene glycol, whose anodic decomposition has also been thoroughly investigated [41-46], was examined as well.

2. Experimental Procedure

Experiments were carried out using glass beakers (Pyrex) with 60 mm diameter and 35 mm height filled with de-ionized water. Each beaker had a wall strength of 1.5 mm, a 2.2-2.5 mm (diameter) lip around the upper edge and a single spout. The beakers were filled with de-ionized water such that the water surface was about 3 mm below the beaker's edge which resembled, for pure water at room temperature, a mass of 66.0 ± 0.5 g. The initial conductivity of the de-ionized water was $0.055~\mu S~cm^{-1}$ measured with the integrated conductivity/TOC meter of the Millipore A10 TOC type

water supply system (Millipore Corp., Billerica, MA, USA). This value rose quickly to 0.4 - 1.0 µS cm⁻¹ depending on the atmospheric conditions and storage time in a dark glass bottle. The pH value of the water was around 5 due to CO₂ saturation and a TOC amount of three ppb. For pH estimations a Merck pH-Box paper (pH 1-10, Art. Nr. 109526) was used. For conductivity measurements, a conductivity meter 3210 from WTW (Wissenschaftlich-Technische Werkstätten Weilheim, Germany) was used, which was calibrated by the manufacturer and had a measurement range from 0.01 - 200 µS cm⁻¹. For all experiments thin platinum plates (2.5×2.5 cm², 0.5 mm thickness) were used as electrodes. These plates were placed in the rear part of the beakers so that the distance between the electrodes was ~12 cm. The aqueous bridges were created by positioning the beakers' spouts pointing at each other in line with the electrodes.

The power was provided by a FUG HCP 350-65000 (serial no.: 161119-01-01, FUG Elektronik GmbH, Rosenheim, Germany) with the dc output stable up to 5 mA and the voltage continuously adaptable up to 70 kV with a waviness smaller than 0.05% and a 0.1 kV accuracy. The operating voltage of the floating water bridge varied between 5 kV and 20 kV at a current of 0.5 mA. In all experiments, the anode (+ pole, high voltage) was on the left, the cathode (- pole, ground) on the right. For imaging, a Panasonic HDC-SD100 camera with a 2.95 - 35.4 mm lens was used. All images were scaled. With this scaling and the above macro lenses, the bridge diameter and length were measured within ± 0.2 mm accuracy (± 0.1 mm at each side). To record the mass flow through the water bridge both beakers rested on electronic scales (EW 1500-2M, Kern, Balingen, Germany), each equipped with a serial interface with a measurement range of 0 - 1500 g and ±0.01 g accuracy.

The phenol or ethylene glycol stock solution (1 mM, 10 mM) were prepared (phenol for synthesis, Sigma Aldrich, purity: ≥99.9; ethylene glycol, VWR, purity: ≥99%) with de-ionized water (Milli-Q system, $\Omega_{\text{internal}} > 18 \text{ M}\Omega \text{ cm}$) for all experiments and then filled in a clean glass beaker right before the experiment. The beakers were always filled with the same weight of the solutions (measured with a B3001-S balance produced by Mettler Toledo, accuracy: ± 0.1g) before the voltage was applied. Temperature and conductivity of the solutions were measured in both beakers before and directly after the experiment. As soon as the bridge was formed, the beakers were pulled apart to a distance of 1.0 (± 0.1) cm between the spout tips. The average time between the formation and final beaker position was ~35 s. In this time the balances showed high

Table 1. List of conducted bridge experiments.

Nr.	Cathodic beaker		Anodic beaker		Analyses
	substance	conc.	substance	conc.	transport, concentration
1a	phenol	1 mM	water		transport, concentration
1b	water		phenol	1 mM	transport, concentration
2a	phenol	10 mM	water		transport, concentration
2b	water		phenol	10 mM	transport, concentration
3a	phenol	0.53 mM	phenol	0.53 mM	concentration
3b	phenol	5 mM	phenol	5 mM	concentration
3c	phenol	10 mM	phenol	10 mM	concentration
3d	phenol	50 mM	phenol	50 mM	concentration
3e	phenol	100 mM	phenol	100 mM	concentration
3f	phenol	531 mM	phenol	531 mM	SEM, EDX, optical
1a	water		glycol	10 mM	transport, concentration
4b	glycol	10 mM	water		transport, concentration
Ба	glycol	3.6 mM	glycol	3.6 mM	concentration
5b	glycol	11.3 mM	glycol	11.3 mM	concentration
5C	glycol	46 mM	glycol	46 mM	concentration
5d	glycol	450 mM	glycol	450 mM	concentration
ба	bisphenol-A	100 μ g L ⁻¹	water		feasibility
6b	water		bisphenol-A	$100\mu\mathrm{g}\;\mathrm{L}^{\text{-}1}$	feasibility
7a	hydrochinone	50 g L ⁻¹	water		feasibility
7b	water		hydrochinone	50 g L ⁻¹	feasibility
8a	hydrochinone	500 mg L ⁻¹	water		feasibility
3b	water		hydrochinone	500 mg L ⁻¹	feasibility
9a	p-cresol	100 μ g L ⁻¹	water		feasibility
9b	water		p-cresol	$100\mu\mathrm{g}\;\mathrm{L}^{\text{-}1}$	feasibility
0a	p-cresol	100 mg L ⁻¹	water		feasibility
0b	water		p-cresol	100 mg L ⁻¹	feasibility



Figure 1. Stable liquid bridging with deionized water, 10 kV DC, 0.3 mA. Pt electrodes.

fluctuations due to the beaker movement, which are thus not taken into consideration in the consequent graphs and calculations. The experiments carried out are summarized in Table 1. In all experiments, the operating voltage was 10 (\pm 1) kV; the current was ~0.3 mA for concentrated solutions of 1 mM or less, and ~0.75 mA for concentrations of 10 mM or more.

It should be noted that "experiment" does not equal a single measurement but a number of measurements. Six measurement series were carried out with the concentrations of 1 mM (phenol) and 10 mM (phenol, ethylene glycol), in either anodic or cathode beaker with the other beaker filled with pure water (Exp. 1, 2 and 4). The experiments lasted between 60 and 3000 seconds enabling the determination of the solute's concentration and the mass transport as a function of time. The equilibrium experiments (Exp. 3 and 5) were run as long as possible, where bridges using solutions with higher concentrations tended to be less stable than those with lower concentrations. Finally, the feasibility of bridge formation using solutions of bisphenol-A, hydrochinone and p-cresol was investigated (Exp. 6-10). If an unexpected breakdown of the bridge

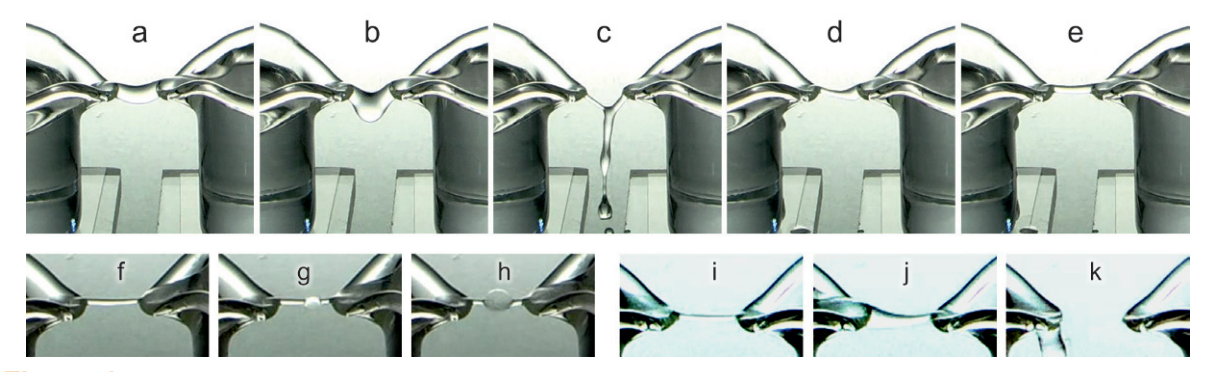


Figure 2. Typical bridge instabilities: leaking bridge (a-e) (0.531 mol L⁻¹ phenol in anode beaker); bubble in bridge (f-h) (50 g L⁻¹ hydrochinone in anode beaker); asymmetric shape and breakdown (i-k) (50 g hydrochinone in cathode beaker)

or visible discharges between the beakers occurred, the experiment was excluded from the evaluation. The detection of the phenol concentration was done using a 'Dr.Lange' quick test with an approximate error of 5 %. Due to the formation of polymeric phenol derivatives on the anode, the electrodes had to be cleaned chemically (conc. $\rm H_2O_2$ and conc. $\rm HNO_3$) after each experiment [37].

The ethylene glycol was quantified using GC-MS (Agilent 6890 GC coupled with a 5973 MSD, Agilent, Waldbronn, Germany) with a polar capillary column consisting of cross-linked polyethylene glycol (Innowax, $30\,\text{m}\times2.5\,\text{mm}\times25\,\mu\text{m}$). The temperature gradient of $80\,^{\circ}\text{C}$ to $260\,\text{C}^{\circ}$ with a heating rate of $10\,^{\circ}\text{C}$ min-1 was used. The temperature of the injector was $250\,^{\circ}\text{C}$. The ionization energy was 70 eV (EI). The selected ion monitoring (SIM) mode was applied. An external calibration in the range of 0.05 to 6 mM was used for the quantification of ethylene glycol. The samples were diluted 10-100 times with water before measurements.

3. Results and Discussion

Stable liquid bridging (see Fig. 1) could be accomplished with solutions of all substances listed in Table 1. If not mentioned otherwise, the temperature change of the beakers was similar to that of pure water [6] starting from 19°C and slowly rising up to ~24°C after the longest measurement time (30 min).

Some of the stable bridges became unstable and/or broke down during the experiments. The most common instability observed was leaking (see Fig. 2a). This also happened to a water bridge if the amount of water in the beakers was too large and/or the current was too high so that bridges with diameter thicker than ~4 mm were formed. Moreover, this kind of instability was also caused by very high concentrations of phenol. Interestingly, high concentrations of hydrochinone caused different instabilities depending on where the substance was

located: When a 50 g L-1 hydrochinone solution was bridged to water in the cathode beaker, sometimes bubbles would form within the bridge (Figs. 2f-h). It should be mentioned here that the bubbles shown in Figs. 2g-h show two separate events and not a time evolution. With the position of the beakers interchanged the shape of the bridge became more cone-like (see Figs. 2i-k) before breaking down.

3.1. Phenol solutions

Previous studies with pure water have shown that there is a general trend of more water flowing into the cathode beaker than vice versa, resulting in an increase of the water level in the cathode beaker until a labile equilibrium is reached [3].

Low concentrations (1 mM L^{-1}) of phenol did not change this behavior.

The concentrations obtained after a series of measurements run for times between 30 and 3060 seconds of a 1 mM phenol solution are shown in Figs. 3 and 4 for transport from anode to cathode and *vice versa*, respectively (exp. 1a and 1b).

The concentration sum (here fitted with a linear slope including 95% confidence and prediction bands) shows that in these experiments the electrochemical decomposition of phenol seems negligible, however, the conductivity measurements clearly indicate a partial decomposition in the anodic beaker (Figs. 5 and 6).

This happened at a faster rate when the phenolic solution was already present at the anode (Fig. 6) than when it had to be transported there (Fig. 5). Interestingly, the conductivity in the cathode beaker seems to decrease – not only when the phenolic solution is present in that beaker (Fig. 5), but also in the case of pure water (Fig. 6). Most probably, this effect has nothing to do with phenol and is a result of electrophoretic transport of the natural HCO₃ and CO₃²⁻ ions [47] to the (positive) anode. A quick test of the pH showed indeed a neutral – basic milieu in the cathode beaker (7-8) and an increased acidity in the anode beaker (4-5).

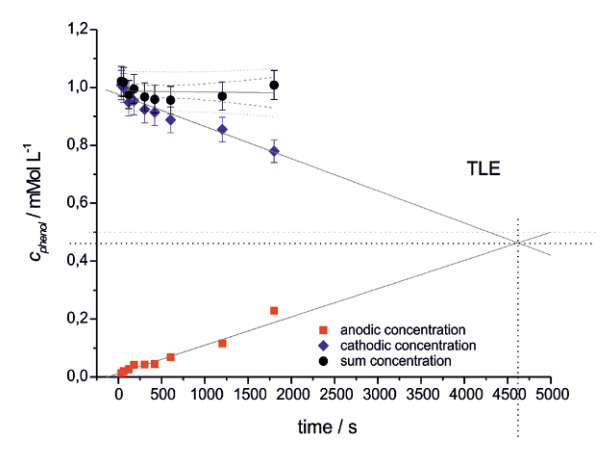


Figure 3. Exp. 1a: Transport of phenol from cathode to anodic beaker. The grey dashed line marks the theoretical mixture concentration (0.5 mmol L¹); the black dashed lines show concentration and time at the theoretical linear equilibrium (TLE). The concentration sum is evaluated with a linear fit including 95% confidence (dashed) and 95% prediction (dotted) intervals.

The linear extrapolations in Figs. 3 and 4 were added in order to obtain the "theoretical linear equilibrium" (TLE), the time when the concentrations in both beakers would be the same provided that only water is transported from the water beaker, and the concentration in the phenol beaker remains the same. Strictly spoken, this is only true for the very first moment of bridging; and due to mixing in the beakers this behavior is in reality rather hyperbolic than linear. However, this extrapolation works well for the purpose of comparison. In case of the 1 mM solutions these times are 4667 s (anode to cathode) and 4623 s (cathode to anode), thus comparable within a 10% error. Furthermore, the theoretical end concentration is slightly above 0.5 mM (the concentration achieved after perfect mixing) in case of the anode to cathode transport, and below 0.5 mM in the cathode to anode experiment. This is due to the fact that in both cases the transport rate from anode to cathode is slightly higher than the flow from cathode to anode which is in general agreement with the mass transport observed in this work and in earlier experiments for pure water [3,6].

Previous experiments revealed mono-directional mass transfer rates between 40 and 280 mg s⁻¹ [6]. In this work we provide additional proof that the mass transport is actually bidirectional, since whereas the phenol concentration is rising in the water beaker, it is declining in the beaker with the phenol solution. This is, for obvious reasons, only possible if a bidirectional flow occurs. The transport rates are of the same order of magnitude as the mono-directional ones observed with water [6], namely up to 182 mg s⁻¹ when calculated from the actual weight, and up to 103 mg s⁻¹ when calculated from the concentration differences.

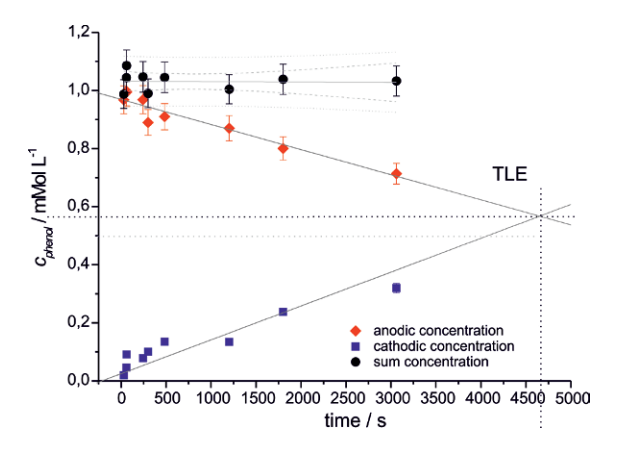


Figure 4. Exp. 1b: Transport of phenol from anodic to cathode beaker. The grey dashed line marks the theoretical mixture concentration (0.5 mmol L¹); the black dashed lines show concentration and time at the theoretical linear equilibrium (TLE). The concentration sum is evaluated with a linear fit including 95% confidence (dashed) and 95% prediction (dotted) intervals.

When looking at the 10 mM series (exp. 2a and 2b) shown in Figs. 7 and 8, the chemical decomposition of phenol is no longer negligible. Here, a significant decline of the concentration sum is observed.

The phenol concentration decreases much faster in the cathode beaker than it increases in the anode beaker, resulting in a steeper decline of concentration sum in this case. The most plausible explanation for this is that a part of the phenol is immediately oxidized once it is transported to the anode. This happens faster when the phenol is transported to the anode (Fig. 8) than when it is already present there (Fig. 7). This seeming contradiction can be explained by the formation of a passivation layer on the anode [39] due to the high phenol concentration. Such a layer obstructs further chemical reactions (see chapter 4 for details on the phenol degradation process). However, if the phenol is transported to this electrode via the EHD flow, which leads from the bridge directly towards the electrode and along its surface downwards into the bulk (see [28] for a detailed description of the lemniscate flow shape), the formation of such a layer is probably hampered both due to the lower overall concentration and due to the flow itself which removes any oxidation products instantly from the electrode surface, and thus electrochemical oxidation processes can happen more easily.

The behavior of the conductivity does not appear to be very regular (Figs. 9 and 10), but as it was the case for the 1 mM concentration, it increases in the anode beaker whereas it decreases in the cathode beaker.

In experiments 2a and 2b the preferred substance transport direction was no longer from anode to cathode, but from water to phenol, as can be seen from

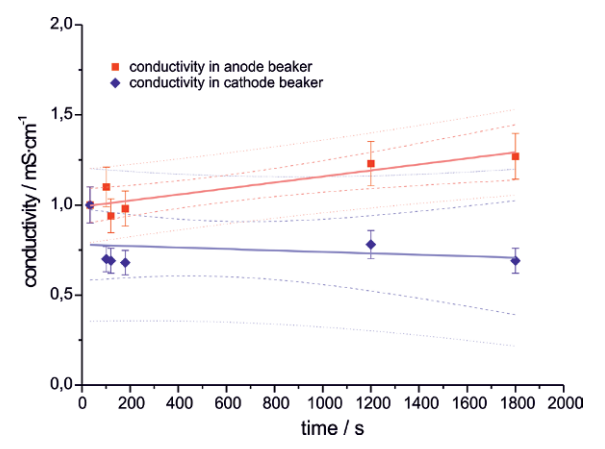


Figure 5. Exp. 1a: Transport of phenol from cathode to anodic beaker, conductivity measurement evaluated with a linear fit including 95% confidence (dashed) and 95% prediction (dotted) intervals.

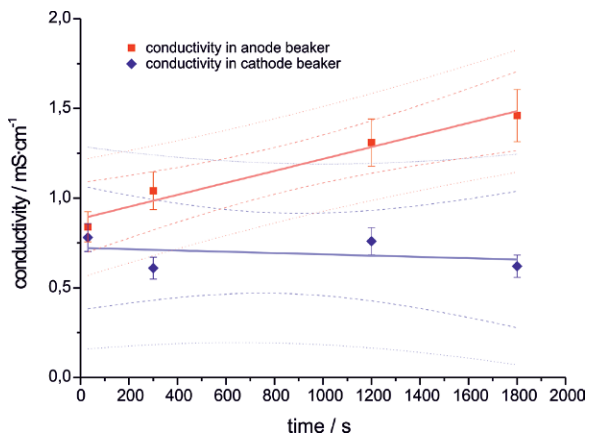


Figure 6. Exp. 1b: Transport of phenol from anodic to cathodic beaker, conductivity measurement evaluated with a linear fit including 95% confidence (dashed) and 95% prediction (dotted) intervals.

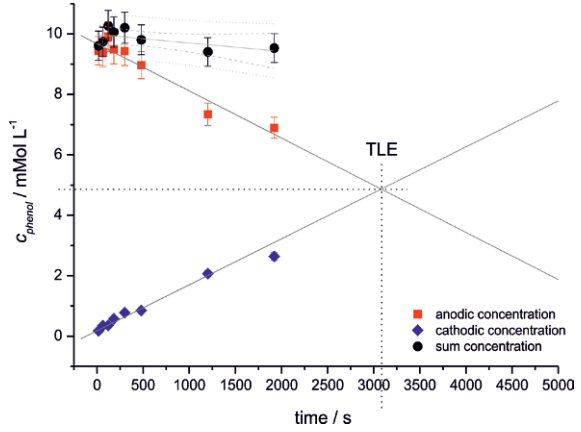


Figure 7. Exp. 2a: Transport of phenol from anode to cathode beaker. The grey dashed line marks the theoretical mixture concentration (5 mmol L-1); the black dashed lines show concentration and time at the theoretical linear equilibrium (TLE). The concentration sum is evaluated with a linear fit including 95% confidence (dashed) and 95% prediction (dotted) intervals.

Figs. 7 and 8 where both TLE concentrations are below 5 mmol L-1. However, this should not be confused with the actual mass transport behavior which remained the same and comparable to that of water [6] with the main flow from anode to cathode – with one exception: For reasons still to be discovered this direction was reversed in one measurement, resulting in more mass in the anode beaker than in the cathode beaker during bridge operation. This exception is compared to a normal mass transport behavior in Fig. 11. The exceptional bridge (orange and cyan lines) started with a mono-directional water flow with rates up to ~ 1000 mg s-1 for a few seconds. After ~5 g of water were transferred (~10 s) the behavior changed to that of a regular phenol bridge (blue and red lines).

The irregularities between 10 and 35 seconds (dotted grey markers) are caused by the beaker separation process on the balances and may not display actual mass changes.

This behavioral pattern could not be repeated since its cause is hitherto unclear; it may not be restricted to the phenol bridge only. A recent work about charge and mass transfer in the water bridge [28] showed that these issues still require some clarification, and future investigations will be aimed at a further understanding of the mass transfer and its directions.

The anode reactions of aqueous phenol solutions in low voltage electrolysis are very well understood and discussed in the literature [32,34,36,39]. Normally, an inhibited electrochemical process takes place on the anodic platinum surface; Gattrell and Kirk [32] showed that the oxidation of phenol to a phenoxy radical- and subsequent quinone- and ether structures at the outer Helmholtz layer is followed by an oxidation of these structures at the inner Helmholtz layer leading to a polymeric film on the anode, carboxylic acids in solution and finally CO₂. The formation of such a layer is common and for low-voltage electrolysis of phenolic solutions (see also [34], [36], [39]) and was also found in the current experiments. Gas formation at the anode could be observed as well, albeit only at very high (Exp. 5f, $c = 50 \text{ g L}^{-1}$) concentrations (see Figs. 12 and 13). The chemical composition determined with EDX revealed a surface composition of 51% Pt, 46% C and 4% O which is consistent with partial covering of the electrode with the polymeric film mentioned above.

The formation of intermediate products can be observed indirectly by the schlieren formation close to the anode (see Figs. 13 b-d) and caused an increase in conductivity, which resulted in an increase of the current necessary to uphold the bridge over time (from 0.3 to 0.75 mA) and thus a relatively larger temperature increase of the solution (from 19°C to 27°C). Moreover,

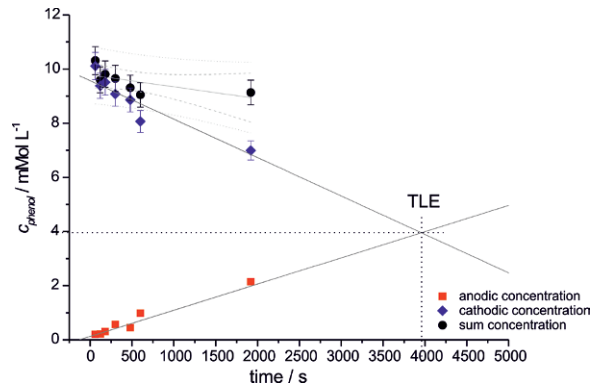


Figure 8. Exp. 2b: Transport of phenol from cathode to anode beaker. The grey dashed line marks the theoretical mixture concentration (5 mmol L¹); the black dashed lines show concentration and time at the theoretical linear equilibrium (TLE). The concentration sum is evaluated with a linear fit including 95% confidence (dashed) and 95% prediction (dotted) intervals.

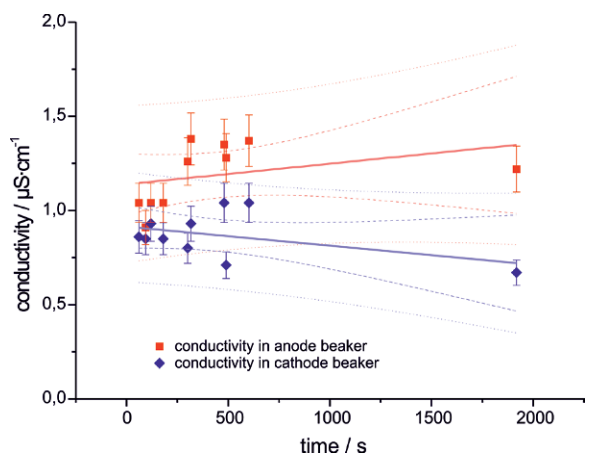


Figure 9. Exp. 2a: Transport of phenol from cathode to anodic beaker, conductivity measurement. The values are evaluated with a linear fit including 95% confidence (dashed) and 95% prediction (dotted) intervals.

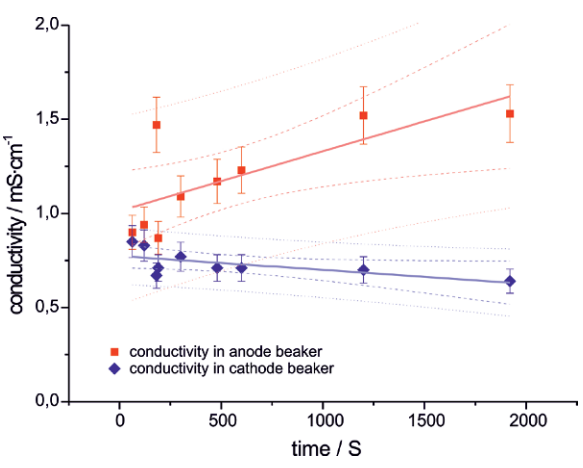


Figure 10. Exp. 2b: Transport of phenol from anodic to cathode beaker, conductivity measurement. The values are evaluated with a linear fit including 95% confidence (dashed) and 95% prediction (dotted) intervals.

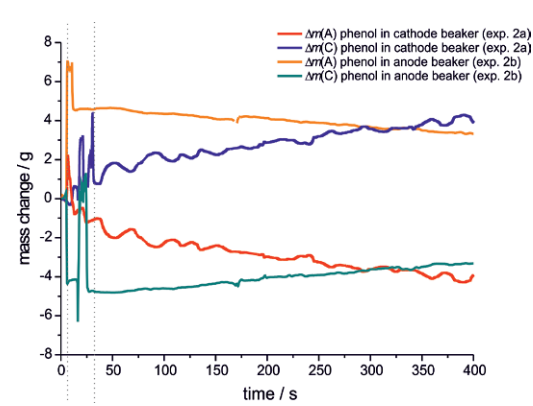


Figure 11. Comparison of the measured mass flow of one exemplary experiment of the series 2a with an extraordinary one of series 2b. The dotted grey lines mark the beaker separation time during which the read out of the balances is partly erroneous.

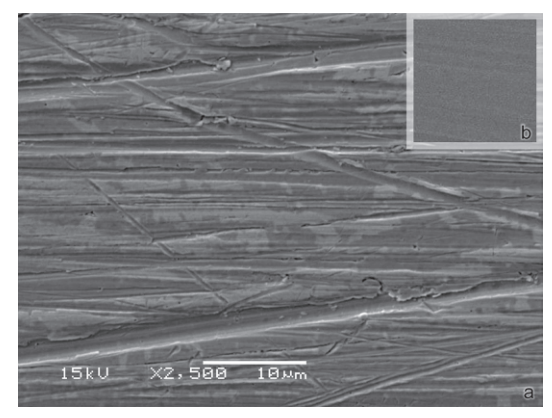


Figure 12. SEM picture of the anodic platinum electrodes after experiment 5f (a, 50 g L⁻¹, 9 kV, 0.75 mA). The insert (b) shows the surface of the clean cathode as comparison (same magnification).

a passivation of the electrode surface as suggested by. Xiao-yan Li et al. [39] could have contributed to the higher current requirement.

The equilibria experiments started with phenol solutions of the same concentrations in both beakers and showed that the concentrations remained constant throughout the experiment, thus no electrophoretic separation occurred (Exp. 3a-3e, see Fig. 14). Small deviations were caused by oxidation/precipitation on the anode as described above. Sometimes, especially at higher concentrations (0.531 mol L-1) a few bubbles appeared after around 5 min on the anode (see also Fig. 13). Since there are no bubbles at the cathode and there is no bubble formation at all when lower concentrations were used, this work confirms the earlier findings [2-6] that electrolysis is not observable. Thus it is safe to assume that the gas formed at the anode is CO₂ due to the degradation of phenol.

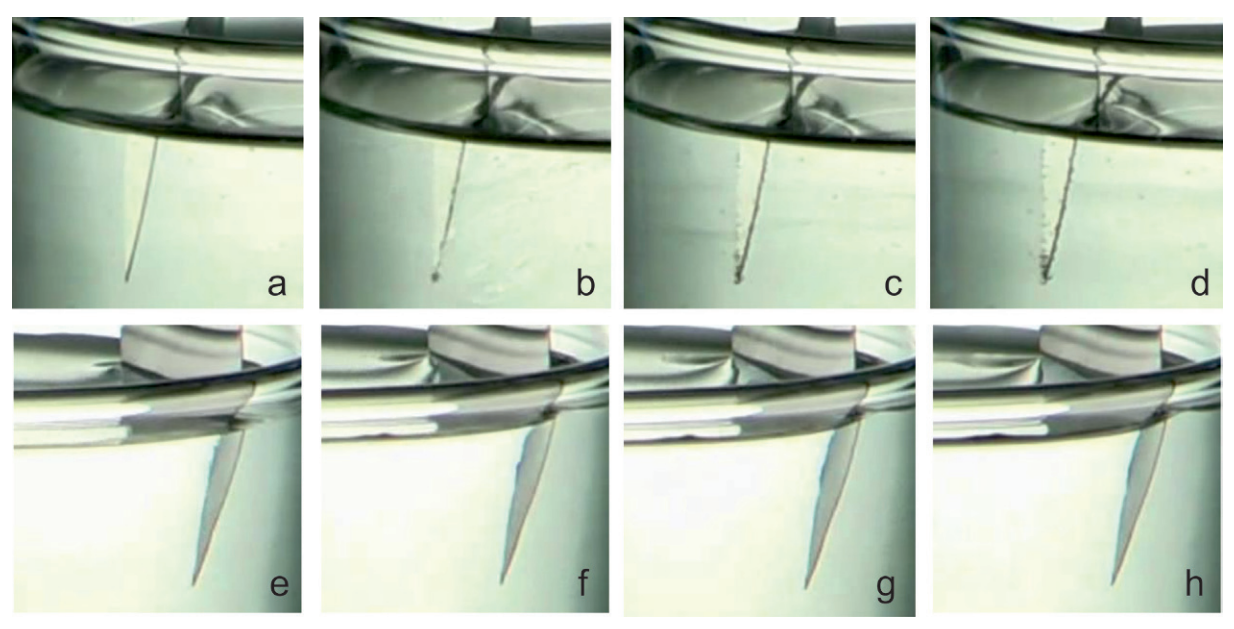


Figure 13. Gas formation over time at the anode (a-d) during experiment 5f (531 mM phenol in both beakers) in comparison to the cathode where no gas formation could be observed (e-h). The pictures were taken after 34 (a,e), 94 (b,f), 214 (c,g) and 274 s (d,h), respectively.

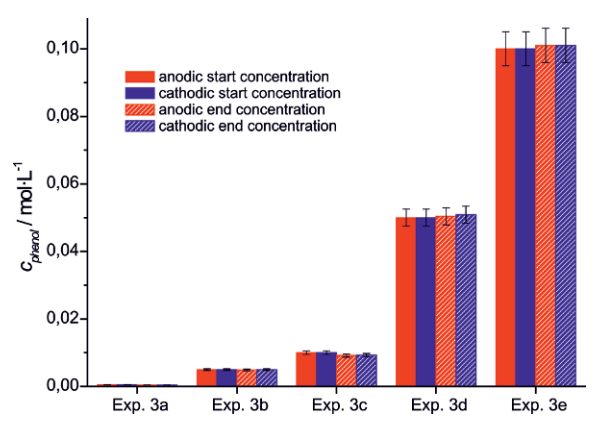


Figure 14. Concentration comparison after the equilibria experiments (3a-3e). The bridges were run for 600 s except Exp. 3c which was run for 580 s.

3.2. Ethylene alycol solutions

In contrast to phenol, ethylene glycol derivatives do not easily polymerize, thus neither the anode nor cathode showed any precipitates. The concentration and conductivity behavior was comparable to that of phenol of the same concentration (Exp. 2b, Figs. 7 and 8) and is shown in Figs. 15 and 16.

In Fig. 15 the concentration sum seems to increase over time. Naturally, this is impossible since the start concentration for all measurements was 10 mM. However, all sum values are within the measurement precision of 5%, thus the concentration sum can and will be considered as constant.

The behavior of the 10 mmol L⁻¹ glycol solution is comparable to that of the phenol solution with the same

concentration. The TLE times differ significantly, and the TLE concentrations are below the optimum mixture concentration (5 mmol L-1) for both experiments (4a, 4b). As it is the case for phenol the concentration of glycol decreases more rapidly in the cathode beaker than it increases in the anode beaker (Fig. 16) resulting in a decline of the concentration sum, whereas this is not the case when glycol is transported from anode to cathode beaker (Fig. 15). The explanation for this behavior is also similar to that for phenol: Here, electrode poisoning may happen once a significant amount of formate [42] is formed on the anode surface - and again, this is much more likely to happen when the anode is all the time surrounded by glycol molecules - and much less likely to happen when the glycol is transported to the anode and any products like, e.g. formate or oxalate, are immediately removed by the EHD flow and diluted into the bulk. Details on the electrolytic glycol degradation are given in the next chapter.

The conductivity behavior is different from that of the phenol solution. In case of exp. 4a (Fig. 17) the conductivity of the anode beaker is slowly rising since it is being diluted by water, whereas the conductivity in the cathode beaker is decreasing, since the glycol content is increasing.

When looking at exp. 4b, the general trends are the same with the starting conductivities being reversed. This suggests that although glycol is transported towards the anode, the conductivity rises.

Actually, this is not true for short times, as can clearly be seen from Fig. 18. Only after ~120 seconds the

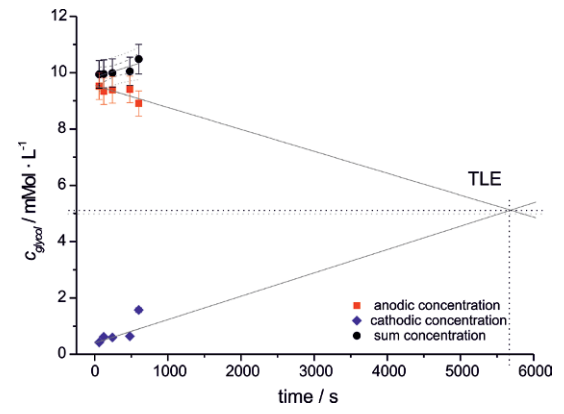


Figure 15. Exp. 4a: Transport of glycol from anode to cathode beaker. The grey dashed line marks the theoretical mixture concentration (5 mM); the black dashed lines show concentration and time at the theoretical linear equilibrium (TLE). The concentration sum is evaluated with a linear fit including 95% confidence (dashed) and 95% prediction (dotted) intervals.

chemical degradation of glycol is more important than the decrease due to the mixture of water with glycol, and the conductivity rises. As it was the case for all experiments, the conductivity in the cathode beaker slowly decreases, suggesting again that the transport of naturally dissolved carbonate and bicarbonate to the anode is the most important process responsible for that. As it was the case for the phenol solutions, a quick pH paper test confirmed this assumption (basic-neutral pH in the cathode, acidic pH in the anode beaker).

The equilibria experiments with glycol showed that the concentrations remained constant throughout the experiments, thus no electrophoretic separation occurred (Exp. 5a-5e, see Fig. 19) as it was also the case for phenol solutions. Small deviations occurred probably due to oxidation on the anode described above or are within the measurement error and thus not significant.

4. Electrochemistry aspects

4.1 General

Since no gas formation was observed during the experiments with lower solute concentration, it is assumed that the electrochemical pathway which leads to CO_2 formation is (partly) inhibited. In a first approximation it can be stated that without any electrolyte added an organic degradation is more difficult than with an electrolyte. The influence of the CO_2 concentration of the surrounding atmosphere on the bridge has been reported earlier [3] showing that a CO_2 increase lead to immediate destabilization and consequent destruction of the water bridge. This indicates that in an EHD bridge set-up the CO_2 solubility of the water is increased

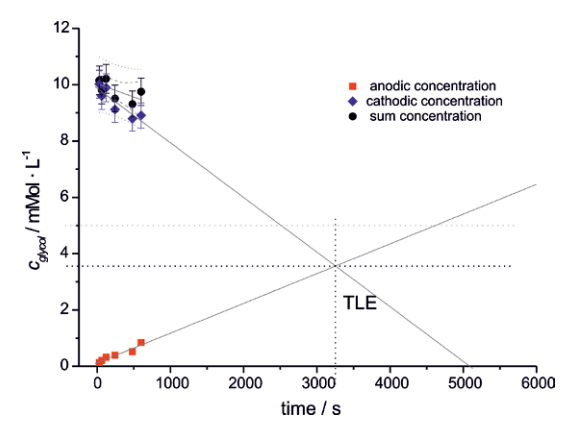


Figure 16. Exp. 4b: Transport of glycol from cathode to anode beaker. The grey dashed line marks the theoretical mixture concentration (5 mM); the black dashed lines show concentration and time at the theoretical linear equilibrium (TLE). The concentration sum is evaluated with a linear fit including 95% confidence (dashed) and 95% prediction (dotted) intervals.

which could thus be a reason for the absence of bubble formation in the present experiment. It is also likely that dissolved CO_2 is concentrated in the anode beaker due to lower pH and a higher conductivity. A detailed analysis of the pH value and the behavior of pH dyes in an EHD bridge is discussed elsewhere [28] and corroborates this assumption, since even with pure water there is a slight pH difference after bridge operation with a slightly lower pH in the anode beaker (5) compared to the cathode beaker (6).

The solution on the anodic side was always a few degrees warmer than the cathode side after the experiment, partly due to the fact that more chemical reactions took place in that beaker. However, the temperature increases were the same for phenol and ethylene glycol solutions as well as for pure water where presumably no electrochemical reactions occur [4,28]. Thus, the more prominent effect here seems to be purely physical: After reaching a labile equilibrium [4], there is less water in the anodic beaker than in the cathode beaker, and a constant flow of hot water in both directions is established. Thus, a smaller volume (the anodic beaker) heats up more quickly than a larger volume (the cathode beaker) when sustained by the same heat source - the bridge.

4.2 Anodic phenol oxidation

There are three known pathways for phenol oxidation on an electrode discussed by Canizares *et al.* [40]:

- a. A direct electrochemical "cold combustion": $Pt(OH \cdot) + R \rightarrow mCO_2 + nH_2O + Pt$, which is catalyzed by physisorbed hydroxyl radicals on a metal surface yielding water and carbon dioxide (*complete oxidation*).
 - b. The "indirect" chemical oxidation in which

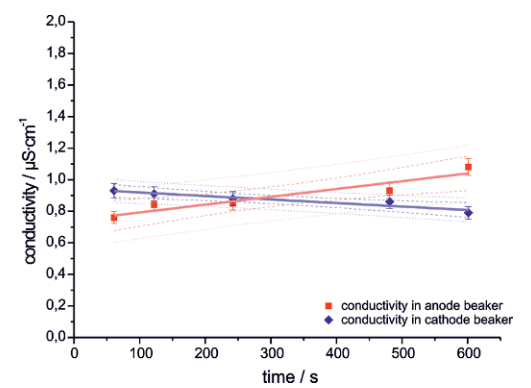


Figure 17. Exp. 4a: Transport of glycol from anode to cathode beaker, conductivity measurement evaluated with a linear fit including 95% confidence (dashed) and 95% prediction (dotted) intervals.

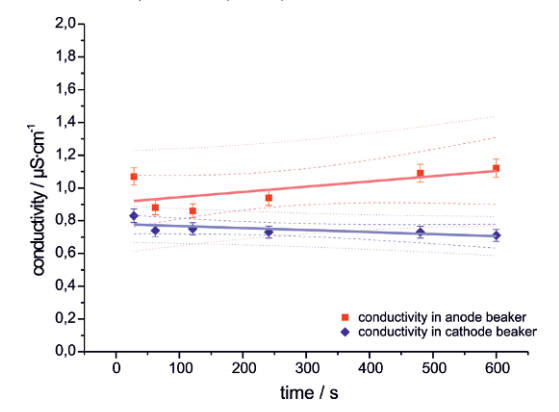


Figure 18. Exp. 4b: Transport of phenol from cathode to anode beaker, conductivity measurement. The values are evaluated with a linear fit including 95% confidence (dashed) and 95% prediction (dotted) intervals.

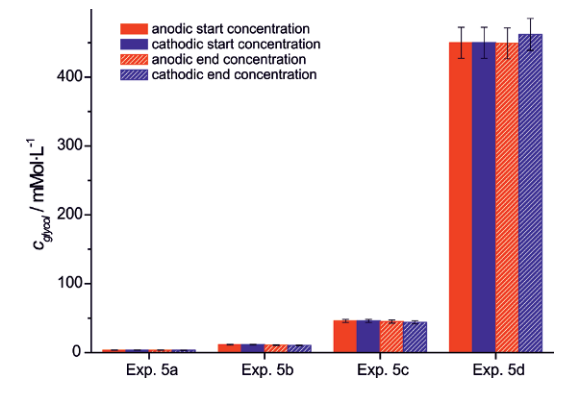


Figure 19. Concentration comparison after the equilibrium experiments (5a-5e). The bridges were run for 600 s except Exp. 5c which was run for 250 s.

chemisorbed hydroxyls selectively produce phenol intermediates via a heterogeneously catalyzed oxidation at the electro-oxidized active sites [40] (partly oxidation).

c. An electrophilic attack of hvdroxyl on phenol, $C_6H_5(OH) + OH \stackrel{\longrightarrow}{} C_6H_5O \stackrel{\longleftarrow}{} + H_2O \stackrel{\longrightarrow}{}$ polymers, starting a *radical polymerization*. As the polymers formed have

a lower oxidation potential than phenol, they are more easily oxidized to radicals which can interact with each other by forming polymers of higher molecular weights, leading to the development of a passivating film on the surface of the electrode.

The preferred pathway for a platinum/phenol/water system according to Gattrell and Kirk [32] is the indirect oxidation (b). The oxidation rate increases when more active PtOH• sites on the metal surface (inner Helmholtz layer, "IHL") are available since they are catalyzing this process. The number of hydroxyl ions desorbing from the Pt depends on the oxidized products in the outer Helmholtz layer ("OHL", approx. 2 nm from the metal surface [32]), e.g.: phenoxy radicals, benzoquinone, hydroquinone and aromatic radical polymer precursors, which are blocking the OHL reactions and let the IHL reactions predominate. The more reduced Pt sites are available on which OH can adsorb, the higher the oxidation rate of phenol. The polymerization (c) is always active, depending on pH, temperature and current density, thereby decreasing the active electrode surface as a function of time. If phenol directly is adsorbed on the Pt-surface, oxidation is suppressed whereas polymerization can still occur.

In our experiments, a polymeric film on the anode was always formed regardless of the phenol concentration. At the highest concentration used (0.531 mol L-1), gas formation at the electrodes could be observed. These observations allow the following conclusions: Generally, polymerization (c) seems to be the predominant pathway for low concentration experiments, whereas partial and possibly full oxidation may play a role for the higher concentrations.

One has to keep in mind, however, that the quoted pathways and reactions are defined for experiments using voltages approximately 4-5 orders of magnitude lower than in the experiments presented. In low voltage experiments, the complete oxidation of phenol happens directly at the surface (IHL), whereas intermediates and successively polymers are formed a few nanometers away (OHL). When applying high voltage, it is plausible to assume that there might be more than two layers, and that the thickness of these layers is increased. Thus, an expanded OHL would provide more polymerization educts, which precipitate on the anode before direct cold combustion or the indirect chemical oxidation can become relevant.

Alternatively, one could imagine that the IHL layer is constantly depleted due to the dielectrophoretic, macroscopic mass transport to and from the electrode, thus all intermediate products are flushed away from the anode into the diffusion layer before they can decompose to CO₂. This would also explain why the CO₂ formation

starts anyway at a certain phenol concentration after some time, since in this case also the stream flowing toward the electrode might already contain intermediates formed shortly before, which can then be oxidized upon contact with the anode. The lemniscate flow shape reported in [28] allows such a hypothesis.

4.3 Anodic Ethylene Glycol oxidation

According to Christensen and Hamnett [44], the main products of low voltage ethylene electrolysis in acidic environments are glycolic acid and carbon dioxide. This reaction takes place at a relatively small number of active sites, which can be poisoned by carbon monoxide getting terminally bonded to the electrode. In alkali, the main products are glycolate, oxalate and carbonate [44]. De Lima et al. [41] describe also the formation of oxalic acid and formic acid as side products. The production of glycolate and carbonate appears to take place via the same intermediate, but oxalate is apparently produced by further oxidation of desorbed glycolate. Comparable results were found by Matsuoka et al. [42]. which state that in alkaline solutions the oxidation of ethylene glycol on platinum occurs via glycol aldehyde glyoxal- glycolate- glyoxylate- oxalate pathway yielding carbonate and carbon dioxide. According to them an electrode poisoning (formate formation) and a nonpoisoning (oxalate formation) electrochemical pathway in electrooxidation of ethylene glycol exists. Kadirgan et al. [45] describe an adsorption process followed by an inherently concerted interfacial step, or series of steps in alkaline media. The necessary ability of platinum to dissociatively chemisorb organic reactants such as alcohols including ethylene glycol is well known in electrochemical as well as gas phase environments [46], the oxygen-transfer agent on platinum appears to be adsorbed water or hydroxyl species.

When using ethylene glycol solutions in the experiments presented the electrodes remained clean, and no gas formation could be observed. The observed increase in conductivity in the anodic beaker and the decrease in the cathode beaker is, if at all, only slightly higher than that observed in pure water and presumably only due to different pH values (different CO, concentrations from ambient CO₂) in these beakers (see also [28]). However, a partial chemical decomposition is certainly happening when the solution is transported to the anode (see Fig. 16). The interpretation of such an electrochemical behavior can be done in line with that of phenol, just that in this case no polymer precipitates on the electrodes, since the intermediate species are incapable of such a reaction. Any CO2 formed could probably remain in solution and would thus not be observable via bubble formation. Alternatively, the

degradation pathway towards CO_2 could be inhibited by the catalytically favored adsorption of hydroxyl ions on the surface of the electrode and subsequent formation of intermediates (glycolate and oxalate). This hypothesis is also supported by Kelaidopoulou *et al.* [43] who state that the oxidation of ethylene glycol on the electrode surface is shifted to a hydroxyl chemisorption at higher potentials. Moreover, as mentioned in the phenol section (4.2), the electrohydrodynamic mass flow could also disrupt and thus slow down chemical surface reactions significantly – or even prevent them completely.

5. Conclusions

In this work we report the transport and chemical reactions of phenol and ethylene glycol solutions in a special electrohydrodynamic environment, a "floating water bridge" set-up. Thereby, the substances are transported in both directions. The electrochemical activity is significantly higher when the solute is transported from the cathode beaker to the anode beaker, since passivation and electrode poisoning are in this case reduced due to the EHD flow. Phenol gets partially oxidized and polymerized at the anode, a complete decomposition resulting in CO, (bubble) formation is only observed at high concentrations. This can be due to an extension of the outer Helmholtz layer due to the extremely high potential, and/or to the depletion of the inner Helmholtz layer which is caused by the EHD water flow.

No precipitation, but indications for the formation of intermediate species of the full oxidation cycle could be detected when an ethylene glycol solution was used. The conductivity change in the beakers indicates that once phenol and ethylene glycol get oxidized at the anode, the generated species hardly pass the bridge to the other beaker. They seem to be 'expelled' from the lemniscate shaped flow [28] and are concentrating over time in regions of the anode beaker which do not take part in the EHD flow to the cathode. Naturally dissolved CO_2 or other ions which contribute to the conductivity of the solution also share this fate, since the conductivity in the cathode beaker decreased over time during all experiments conducted.

In summary, the experiments presented demonstrate that an EHD environment with a floating liquid bridge set-up provides interesting new possibilities for (electro-) chemical reactions. For future studies, the authors plan to examine these possibilities further by extending the research into the investigation of both other solvents and solutes.

Acknowledgments

This work was performed in the TTIW-cooperation framework of Wetsus, Centre of Excellence for Sustainable Water Technology (www.wetsus.nl). Wetsus is funded by the Dutch Ministry of Economic Affairs, the European Union Regional Development Fund, the Province of Fryslân, the City of Leeuwarden and the EZ/Kompas program of the "Samenwerkingsverband Noord-Nederland". The financial support of both the Applied Water Physics Theme of Wetsus and "Holding Graz" is thankfully acknowledged. The authors would like to thank the whole research team and staff of WETSUS, especially Luewton L.F. Agostinho, Cees Kamp and Adam D. Wexler; as well as Lukasz Piatkowski (AMOLF, Amsterdam). With great pleasure, the authors furthermore wish to thank Profs. Artem Aerov (Physics Department, Moscow State University),

Huib Bakker (AMOLF, Amsterdam), Eshel Ben-Jacob (Tel Aviv University), Cees Buisman (Wetsus - Centre of Excellence for Sustainable Water Technology), Friedemann Freund (SETI Insitute, California), Karl Gatterer (Graz University of Technology), Emilio Del Giudice (Universitá di Milano), Ernst Lankmayr (Graz University of Technology), Jan C.M. Marijnissen (Delft University of Technology), Laurence Noirez (Laboratoire Léon Brillouin, CEA-CNRS/IRAMIS, CEA-Saclay), Gerald H. Pollack (University of Washington), Alan Soper (Rutherford Appleton Laboratories, ISIS, Oxford, UK), José Teixeira (Laboratoire Léon Brillouin, CEA-CNRS/ IRAMIS, CEA/Saclay), Giuseppe Vitiello (Universitá degli studi di Salerno), John Watterson (Ashmore, Australia), and Jakob Woisetschläger (Graz University of Technology) for the ongoing discussion on the water bridge phenomenon (in alphabetic order).

References

- [1] W.G. Armstrong, The Electrical Engineer 10, 154 (1893)
- [2] E.C. Fuchs, J. Woisetschläger, K. Gatterer, E. Maier, R. Pecnik, G. Holler, H. Eisenkölbl, J. Phys. D: Appl. Phys. 40, 6112 (2007)
- [3] E.C. Fuchs, K. Gatterer, G. Holler, J. Woisetschläger, J. Phys. D: Appl. Phys. 41, 185502 (2008)
- [4] E.C. Fuchs, B. Bitschnau, J. Woisetschläger, E. Maier, B. Beuneu, J. Teixeira, J. Phys. D: Appl. Phys. 42, 065502 (2009)
- [5] E.C. Fuchs, P. Baroni, B. Bitschnau, L. Noirez, J. Phys. D: Appl. Phys. 43, 105502 (2010)
- [6] J. Woisetschläger, K. Gatterer, E.C. Fuchs, Exp. Fluids 48, 121 (2010)
- [7] H. Nishiumi, F. Honda, Res. Let. Phys. Chem. (2009) art. ID 371650
- [8] M. Tello, R. Garcia, J.A. Martín-Gago, N.F. Martínez, M.S. Martín-González, L. Aballe, A. Baranov, L. Gegoratti, Advanced Materials 17, 1480 (2005)
- [9] T. Cramer, F. Zerbetto, R. Garcia, Langmuir 24, 6116 (2008)
- [10] A. Widom, J. Swain, J. Silverberg, S. Sivasubramanian, Y.N. Srivastava, Phys. Rev. E 80, 016301 (2009)
- [11] A. Castellanos, Electrohydrodynamics, International Centre for Mechanical Sciences, CISM Courses and Lectures No.380 (Springer, Wien, New York, 1998) ISBN 3-211-83137-1
- [12] J. Mrázek, J. V. Burda, J. Chem. Phys. 125, 194518 (2006)
- [13] W.L. Jorgensen, J. Tirado-Rives, PNAS Proc. Natl. Acad. Sci. 102, 6685 (2005)

- [14] E. Del Giudice, Journal of Physics: Conf. Ser. 67, 012006 (2006)
- [15] T. Head-Gordon, M.E. Johnson, PNAS Proc. Natl. Acad. Sci. 21, 7973 (2006)
- [16] H.E. Stanley, S.V. Buldyrev, G. Franzese, N. Giovambattista, F.W. Starr, Phil. Trans. R. Soc. A 363, 509 (2005)
- [17] C.A. Chatzidimitriou-Dreismann, T.A. Redah, R.M.F. Streffer, J. Mayers, Phys. Rev. Lett. 79, 2839 (1997)
- [18] R. Arani, I. Bono, E. Del Giudice, G. Preparata, International Journal of Modern Physics B 9, 1813 (1995)
- [19] E. Del Giudice, E.C. Fuchs, G. Vitiello, Water (Seattle) 2, 69 (2010) ISSN 2155-8434
- [20] R.C. Ponterio, M. Pochylski, F. Aliotta, C. Vasi, M.E. Fontanella, F. Saija, J. Phys. D: Appl. Phys. 43, 175405 (2010)
- [21] E.C. Fuchs, MDPI Water 2, 381 (2010)
- [22] E.C. Fuchs, L.L.F. Agostinho, A.Wexler, R.M. Wagterveld, J. Tuinstra, J. Woisetschläger, J. Phys. D: Appl. Phys. 44 025501 (2011)
- [23] G.H. Pollack, Cells, gels and the engine of life (Ebener & Sons, Seattle WA, 2001) ISBN 0-9626895-2-1
- [24] K. Ovchinnikova, G.H. Pollack, Langmuir 25(1), 542 (2009)
- [25] H. R. Corti, Langmuir 25(11), 6587 (2009)
- [26] K. Ovchinnikova, G.H. Pollack, Langmuir 25(18), 11202 (2009)
- [27] H.R. Corti, Langmuir 25(18), 11203 (2009)
- [28] E.C. Fuchs, L.L.F. Agostinho, M. Eisenhut, J.

- Woisetschläger, Proc. SPIE 7376, 73761E1 (2010) DOI:10.1117/12.868994
- [29] F. Saija, F. Aliotta, M.E. Fontanella, M. Pochylski, G. Salvato, C. Vasi, R.C. Ponterio, J. Chem. Phys. 133, 081104 (2010)
- [30] A.G. Marin, D. Lohse, Phys. Fluids 22, 122104 (2010)
- [31] A.A. Aerov, Why the Water Bridge does not collapse, arXiv:1012.1592v1 (2010)
- [32] M. Gattrell, D.W. Kirk, J. Electrochem. Soc. 140(6), 1534 (1993)
- [33] B. Fleszar, J. Ploszynska, Electrochimia Acta 30(1), 31 (1985)
- [34] D. Fino, C. Carlesi Jara, G. Saracco, V. Specchia, P. Spinelli, J, Appl, Electrochem. 35, 405 (2005)
- [35] Ch. Comminellis, C. Pulgrain, J. Appl. Electrochem. 21, 703 (1991)
- [36] S. Andreescu, D. Andreescu, O.A. Sadik, Electrochem. Comm. 5, 681 (2003)
- [37] R.C. Kolle, D.C. Johnson, Anal. Chem, 51(6), 741 (1979)

- [38] R. Menini, Y.M. Henuset, J. Fournier, J. Appl. Electrochem. 35, 625 (2005)
- [39] X.-Y. Li, Y.-H. Cui, Y.-J. Feng, Z.-M. Xie, J.-D. Gu, Water Res. 39, 1972 (2005)
- [40] P. Canizares, J.A. Domínguez, M.A. Rodrigo, J. Villaseñor, J. Rodríguez, Ind. Eng. Chem. Res. 38(10), 3779 (1999)
- [41] R.B. de Lima, V. Paganin, T. Iwasita, W. Vielstich, Electrochimica Acta 49, 85 (2003)
- [42] K. Matsuoka, Electrochimica Acta 51, 1085 (2005)
- [43] A. Kelaidopoulou, E. Abelidou, A. Papoutsis, E.K. Polychroniadis, G. Kokkinidis, J. Appl. Electrochem. 28, 1101 (1998)
- [44] P.A. Christensen, A. Hamnett, J. Electroanal. Chem. 260, 341 (1989)
- [45] F. Hahn, B. Beden, F. Kadirgan, Electrochimica Acta. 23, 299 (1978)
- [46] R. Parsons, T. VanderNoot, J. Electroanal. Chem. 257, 9 (1988)
- [47] J. Kendall, J. Am. Chem. Soc. 38, 1480 (1916)